JTTEE5 8:576-582

Particle Velocity and Deposition Efficiency in the Cold Spray Process

D.L. Gilmore, R.C. Dykhuizen, R.A. Neiser, T.J. Roemer, and M.F. Smith

(Submitted 1 December 1998; in revised form 21 May 1999)

Copper powder was sprayed by the cold gas-dynamic method. In-flight particle velocities were measured with a laser two-focus system as a function of process parameters such as gas temperature, gas pressure, and powder feed rate. Mean particle velocities were uniform in a relatively large volume within the plume and agreed with theoretical predictions. The presence of a substrate was found to have no significant effect on in-flight particle velocities prior to impact. Cold-spray deposition efficiencies were measured on aluminum substrates as a function of particle velocity and incident angle of the plume. Deposition efficiencies of up to 95% were achieved. The critical velocity for deposition was determined to be about 640 m/s for the system studied.

Keywords cold spray, deposition, gas dynamic, high velocity, solid state

1. Introduction

The cold gas-dynamic spray method (CGSM), hereafter referred to simply as cold spray, is a relatively new process by which coatings of ductile materials (or composite materials with significant ductile phase content) can be produced without significant heating of the sprayed powder. There is no evidence in the available literature of impact-induced melting. Recent simulations of the impact of single copper particles onto stainless steel substrates suggest that peak interfacial temperatures remain well below the melting point of either material. However, the kinetic energy of the particles is sufficient to produce large deformations and high interfacial pressures and temperatures, which appear to produce a solid-state bond (Ref 1).

Cold-spray processing was developed in the former Soviet Union more than a decade ago as an offshoot of supersonic wind tunnel testing (Ref 2-4). Research in the United States has been conducted so far through a consortium of companies organized by the National Center for Manufacturing Sciences (NCMS) (Ref 5-7). The current investigation is a follow-up to recent efforts to model the aerodynamics of the supersonic flow of the particles in the converging-diverging spray nozzle (Ref 8). In-flight particle velocities were measured at various positions in the spray plume for a range of gun-inlet pressures and temperatures. Deposition efficiencies were also measured as functions of particle velocity and gun-substrate angle.

2. Experimental Procedures

Figure 1 shows a schematic of the experimental setup used in this work. This device is very similar to that used previously by NCMS researchers (Ref 5). The converging-diverging gun nozzle was manufactured out of tool steel and contains a 2 mm diameter circular throat. The exit aperture is rectangular, 2 by 10 mm. The distance between the throat and exit aperture is 80 mm, and the nozzle expands linearly in one dimension.

A Praxair Thermal Spray Products (Appleton, WI) Model 1270 HP computerized high-pressure powder hopper, using

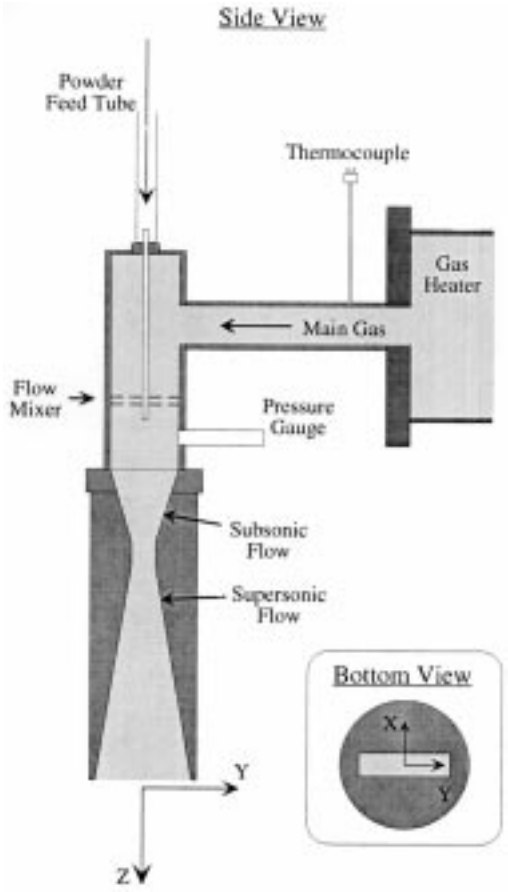

Fig. 1 Schematic of experimental setup indicating reference axes. Not to scale

D.L. Gilmore, R.C. Dykhuizen, R.A. Neiser, and **M.F. Smith,** Sandia National Laboratories, Albuquerque, NM 87185-1130; and **T.J. Roemer,** Ktech Corporation, Albuquerque, NM 87106-4265. Contact e-mail: dlgilmo@sandia.gov.

standard high-pressure gas fittings and equipped with an ultrafine powder wheel, was used to feed the powder. The powder was fed axially into the gun nozzle 25 mm upstream of the throat. The feed tube had an inside diameter of 2.2 mm. The hopper was elevated above the gun, with a wheel rotational speed of 1.0 rpm unless otherwise noted. The powder carrier gas pressure was held 69 kPa (10 psi) above the main gas pressure in order to improve the feed of the fine powders used. All pressures in this article are reported relative to the local atmospheric pressure at Sandia National Laboratories in Albuquerque, NM, approximately 83 kPa (0.82 atm, 12 psi).

The temperature of the main gas flow prior to entering the gun was measured with a type K flow-through thermocouple and was varied between 25 and 500 °C with a simple resistance heater. The powder carrier gas was not heated. Although it is possible to use a powder gas that is different from the main driver gas, in this work the gases were of the same type for a given run, with dry air used in some experiments and helium used in others.

The velocity of a powder particle in a gas flow should vary inversely with the square root of the particle diameter (Ref 8), and thus, finer powders should have higher impact velocities for a given set of spray parameters. However, in practice, difficulty in feeding very fine powders usually limits the minimum size that can be sprayed. All results in this article are for a spherical, gas-atomized copper powder (ACuPowder International, LLC No. 500A, Union, NJ). Two lots were used, one with a volumetric mean diameter of 19 μm and the other a mean of 22 μm. The volume-weighted size distributions, as measured by a laser diffraction system (Model LS-100, Coulter Corp., Miami, FL), are summarized in Table 1, and the powder morphology can be seen in Fig. 2. The oxygen content of the powder was 0.336 ± 0.008 wt%. Particle velocity data were acquired with a laser two-focus (L2F) velocimeter (Polytec Optronics, Inc., Costa Mesa, CA) (Ref 9). The depth of focus for the L2F is approximately the same as the width of the spray plume upon exiting the gun nozzle (2 mm), so some variance from theoretical calculations of centerline behavior can be expected. Gas velocities were not measured.

Deposition efficiencies were measured on 51 by 51 by 3 mm thick grit-blasted aluminum substrates (6061 T6). The substrates were cleaned with an acetone bath followed by a methanol bath, air dried, and then weighed on a digital electronic balance (Model PC 180, Mettler Instrument Corp., Hightstown, NJ). The substrates were weighed again after spraying to calculate the weight gain. Deposition efficiency was calculated as the weight gain divided by the product of the calibrated mass feed rate and the spray time on the substrate. No allowance was made for the weight of substrate material that might have been removed during spraying, as this was generally far less than the weight of the deposited coating. Deposition efficiencies were measured as functions of substrate impact angle and particle velocity. Particle velocities were varied by changing the temperature and pressure of the driving gas. The standoff distance used for the formation of deposits was 25 mm. Compared with in-flight particle characteristics for most thermal spray systems, the in-flight particle characteristics for the cold-spray process change very little with varying standoff distance, as described in this article.

Table 1 Powder size distributions

Volumetric mean diameter	Powder size distribution, μm				
	10%	25%	50%	75%	90%
19 μm	25.9	22.7	18.7	14.5	10.9
22 μm	28.5	25.6	22.2	18.2	14.4

3. Results and Discussion

3.1 In-Flight Particle Velocities

Figure 3(a) displays the variation of mean particle velocity and count rate along the *y*-axis, at a distance of 25 mm from the

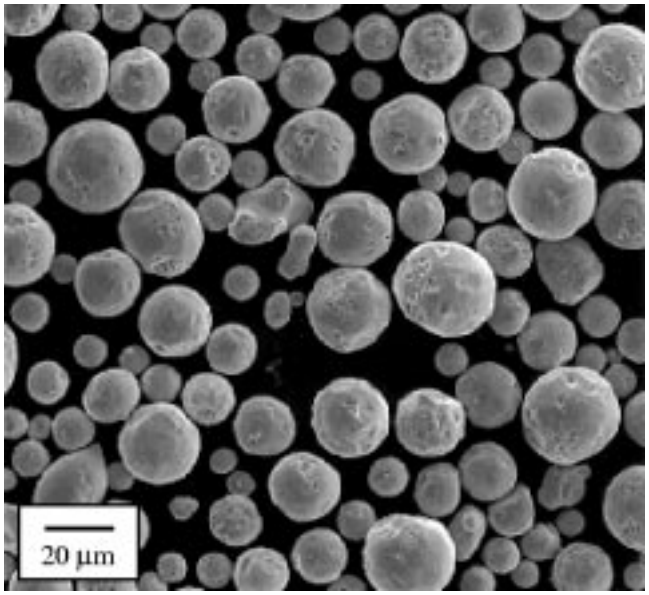

(a)

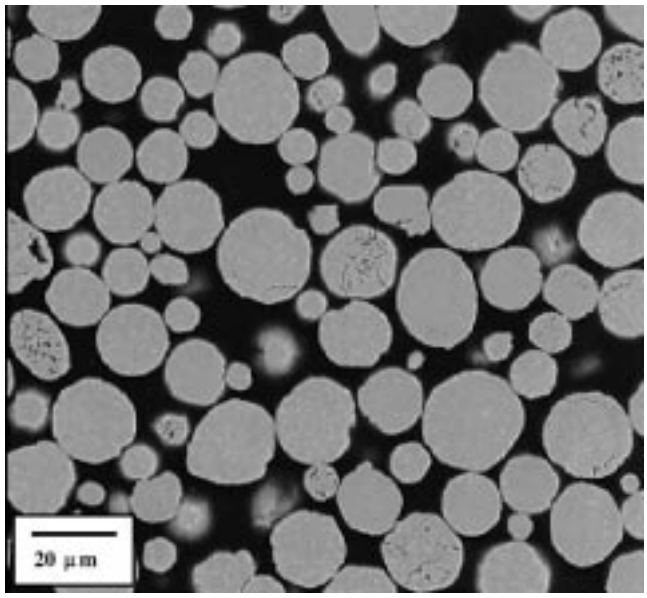

(b)

Fig. 2 (a) Scanning electron microscope (SEM) image of gas-atomized copper powder used in experiments (22 μm mean diameter). (b) SEM image of powder cross section, indicating near full density (22 μm mean diameter)

gun exit (orientation shown in Fig. 1). The velocities vary only 5% over a region that corresponds to roughly two-thirds of the nozzle exit width. Similar velocity distributions were observed at 10 mm from the gun exit. The corresponding particle frequency counts along the *y*-axis drop off significantly away from the central axis of the jet, as might be expected with axial powder injection. Thus, the vast majority of the particles reside in the constant velocity region.

Figure 3(b) shows the variation in mean particle velocity and the count rate along the *x*-axis. Although the velocity drop-off is somewhat steeper than that observed along the *y*-axis, mean particle velocities at the edge of the plume are still greater than 85% of those in the center. Differences between the peak particle velocities and frequencies in Fig. 3(a) and (b) can be due to minor misalignment of the gun or merely due to random fluctuations. The data plotted in Fig. 3 are for helium as the driving gas. Similar profiles were observed with air as the driving gas, although the corresponding velocities were significantly lower, as is explained in further detail in this article.

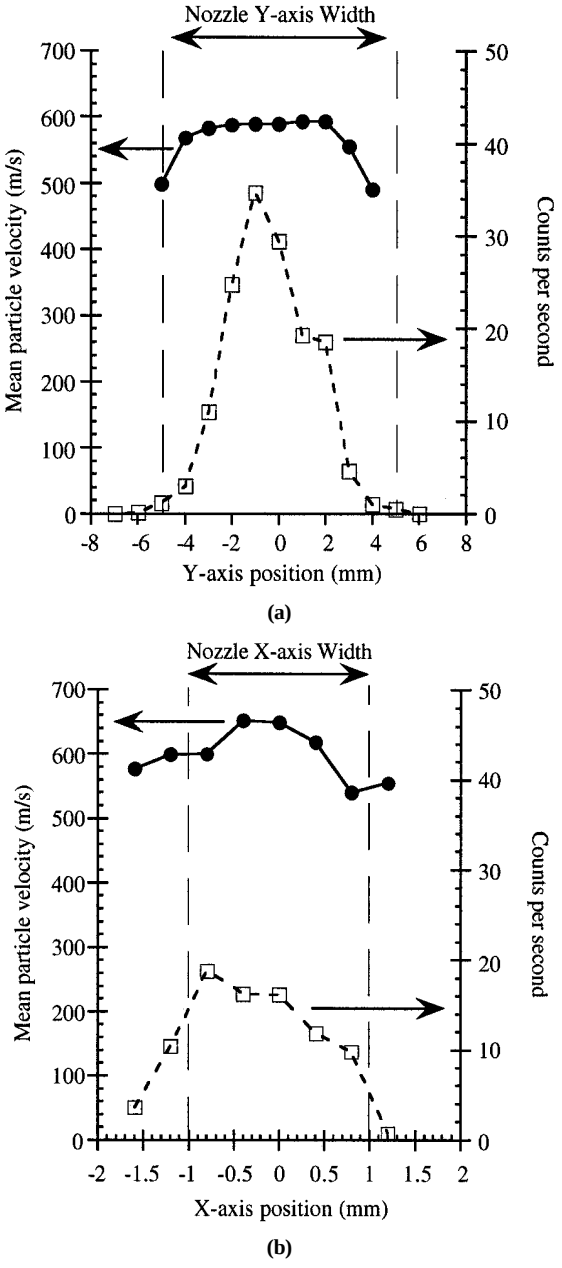

Fig. 3 (a) Mean particle velocity and counts versus *y*-axis position ($x = 0, z = 25$ mm). 19 μm copper powder; 25 °C, 2.1 MPa (300 psi) helium driving gas. (b) Mean particle velocity and counts versus *x*-axis position ($y = 0$, $z = 25$ mm). 19 μm copper powder; 25 °C, 2.1 MPa (300 psi) helium driving gas

The variation of mean particle velocities with *z*-axis (standoff) distance is shown in Fig. 4. With air as the driving gas and inlet conditions of 2.1 MPa (300 psi) and 200 °C, the particles have been accelerated to their peak velocity, just under 400 m/s, by the time they exit the nozzle. They maintain this velocity almost constant to a distance of 50 mm from the exit plane of the nozzle, past which point the velocity decreases roughly linearly, diminishing by about 3% over the next 50 mm. When helium is used as the driving gas, the particles are still accelerating out to a distance of about 30 mm. Due to the lower density of helium, the drag force on the particles is lower than for air at a given gas velocity relative to the particles. Therefore, the distance required for the particles to reach a given fraction of the velocity of the driving gas (which is the limiting velocity) will be greater for helium than for air.

Theoretical calculations for the conditions shown in Fig. 4 indicate that at the gun exit, the particles will have reached 42% of the gas velocity when helium is used and 62% of the gas velocity when air is used (Ref 8). However, since the helium velocity is 2.5 times that of air, higher particle velocities still are observed with helium as the driving gas.

The flow of a high-velocity gas jet normal to a solid barrier will create a high-pressure region close to the surface. This high-pressure region might be thought to affect the velocity of the in-flight particles. In order to determine if this is the case, L2F velocity measurements were taken at a *z*-axis distance of 8 mm from the gun exit, 2 mm above a substrate, using room temperature (RT) air as the driving gas. These measurements were then

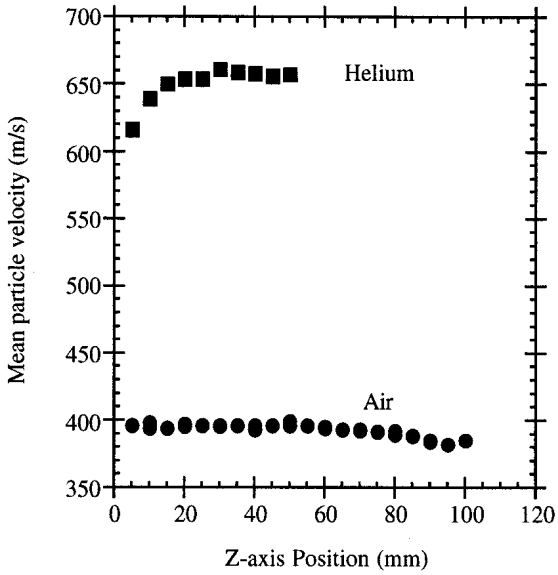

Fig. 4 Mean particle velocity versus *z*-axis position ($x = 0, y = 0$). 22 μm copper powder; 200 °C, 2.1 MPa (300 psi) helium or air driving gas

repeated without the presence of the substrate. Measurements could not be reliably obtained closer to the substrate due to scattering of the laser beam. Figure 5(a) shows that the presence of the substrate has no effect on particle velocity distribution curves measured 8 mm below the gun exit. This result agrees with theoretical modeling that predicts that for a 10 mm standoff distance, the gas jet does not begin to slow significantly until approximately 1 mm above the substrate. For a particle moving at 400 m/s, this leaves less than 3 μs before particle impact, too short a time for the region of stagnant gas to significantly decelerate the powder.

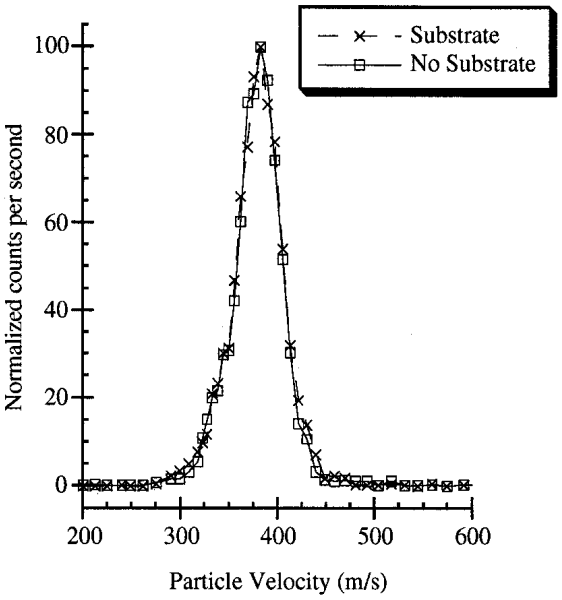

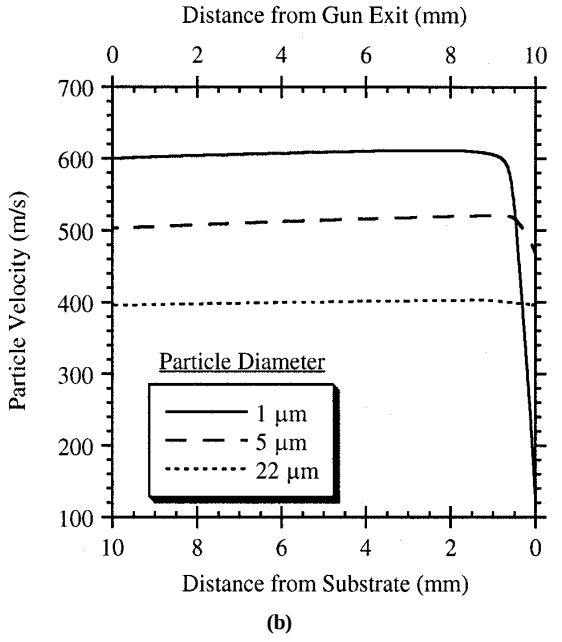

Fig. 5 (a) Particle velocity distributions, with and without substrate. Measurements at $x = 0$, $y = 0$, $z = 8$ mm (2 mm above substrate, when present). 22 μm copper powder at 25 °C, 2.1 MPa (300 psi) air driving gas. (b) Theoretical calculations of particle deceleration near substrate ($x = 0$; $y = 0$) for 10 mm gun standoff, fully dense copper powder at 27 °C with 2.1 MPa (300 psi) air driving gas

Figure 5(b) shows computational fluid dynamics calculations for fully dense copper particles in a flow of air with gun inlet conditions of 2.1 MPa (300 psi) and 27 °C. The calculated gas velocity at the gun exit is 600 m/s. This figure also shows that the particles would need to be smaller than 5 μm in diameter to be slowed by more than 10% before impact. Details of similar calculations can be found elsewhere (Ref 10).

The effect of mass loading on particle velocity was investigated. Figure 6 shows that above about 0.5 g/s, the mean particle velocity decreases linearly with the mass feed rate, which is directly proportional to the powder-hopper wheel rotational speed. The decrease in velocity might be due to the increased mass that the gas flow must accelerate.

Supersonic fluid flow theory predicts that the particle velocities should vary as the log of the gas stagnation pressure (Ref 8). Figure 7 indicates that the experimental data for inlet gas temperatures of 25 and 300 °C are fit well by a logarithmic curve, although the measured values fall slightly below those predicted by the one-dimensional flow theory. This shortfall might be explained in part by the fact that the theoretical values are calculated assuming an isentropic (adiabatic and frictionless) gas expansion in the gun after the throat.

Under real world experimental conditions, obvious energy exchange between the gas and the nozzle walls is observed. For example, when the gun is running without preheating of the main gas, water vapor sometimes condenses on the gun, and when the gun is running with a main gas inlet temperature of 300 °C, the outside of the gun becomes too hot to touch with the bare hand. However, nozzle temperatures were not systematically measured.

Figure 8 indicates the variation in particle velocity that is obtained with changes in gas temperature and gas type at a constant inlet stagnation pressure of 2.1 MPa (300 psi). Switching from

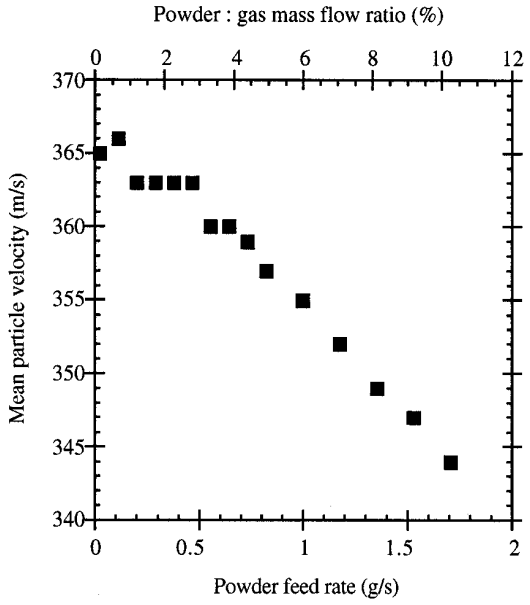

Fig. 6 Mean particle velocity versus mass loading ($x = 0$, $y = 0$, $z = 10$ mm). 22 μm copper powder at 25 °C with 2.1 MPa (300 psi) air driving gas; 805 slpm total gas flow

air to helium for the driving gas results in a large increase in mean particle velocity. This is due to the increase in gas velocity obtained with lower molecular weight gas. Increasing the temperature of the main gas flow also allows higher gas velocities to be achieved for a given pressure (Ref 8, 11). This increase in gas velocity outweighs the corresponding decrease in gas density, so the drag on the particles increases. There is fairly good agreement observed between the experimental velocity measurements and the predicted values, especially for the air data. However, the leveling of the measured particle velocities at higher gas temperatures is not well understood. This effect can be attributed to nonisentropic expansion (as already noted) or to the fact that the unheated powder gas might not be mixing well with the surrounding main gas flow after injection into the gun; that is, the gas conditions in the gun might be significantly different from the well-mixed state assumed for modeling. This effect should be more pronounced at higher temperatures because the main gas flow decreases with temperature for a given pressure, while the powder gas flow remains roughly constant.

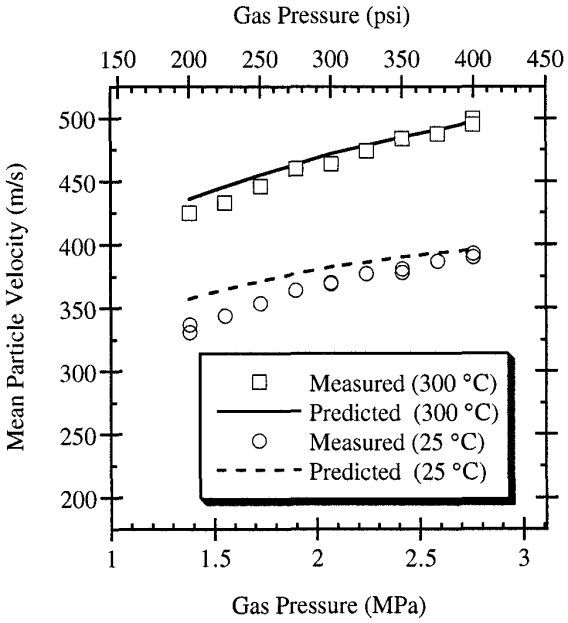

Fig. 7 Mean particle velocity versus gas pressure ($x = 0$, $y = 0$, $z = 10$ mm). 22 μm copper powder; 25 and 300 °C air driving gas

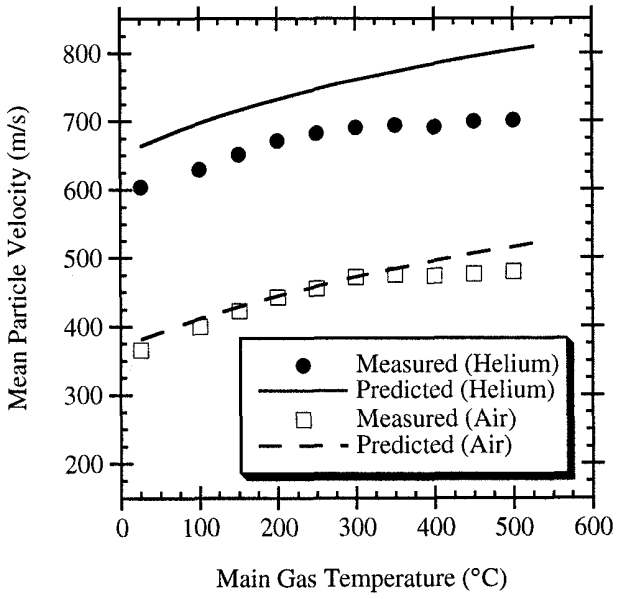

Fig. 8 Mean particle velocity versus temperature ($x = 0$, $y = 0$, $z = 10$ mm). 22 μm copper powder; 2.1 MPa (300 psi) helium or air driving gas

3.2 Coating Deposition

The cold-spray process has been shown to be capable of rapidly applying coatings over large areas (Ref 2, 3). High deposition efficiencies have been reported for some material-substrate combinations, such as copper onto copper (Ref 2). In the current work, coating thicknesses of 4 to 5 mm were found to be easily achievable. No attempt was made to determine if there is an upper limit on coating thickness. The footprint of the spray plume on the substrate at a standoff distance of 25 mm was approximately 12 by 3 mm. The 12 mm width of the coating was consistent with the divergence angle of the nozzle. This observation was supported by L2F observations of in-flight particle trajectories. The oxygen content of the coatings was 0.280 ± 0.005 wt%, somewhat less than that of the starting powder (0.336 ± 0.008 wt%). The cause of this decrease is not known. It might be due to preferential deposition of low oxide-content particles at the expense of high oxide-content particles.

Figure 9(a) shows the effect of mean particle velocity on the deposition efficiency of copper on an aluminum substrate oriented normal to the gun axis at a standoff distance of 25 mm. Particle velocities can be varied by changing the initial pressure and temperature of the driving gas. Since the effective substrate material changes from aluminum to copper as the coating is deposited, it might be expected that there would be a dependence of the deposition efficiency on coating thickness. However, this was not observed in the present work. Data for the deposition of copper on copper and for the deposition of aluminum on copper are also given for comparison (Ref 2, 5). The data presented in this article are similar to earlier data for copper-copper deposition up to approximately 50% deposition efficiency but show considerably higher efficiencies at particle velocities above 700 m/s. Not enough details are available on the experimental set-up or alloy compositions used in the previous work to speculate as to the possible causes for this difference.

It should be noted that mean particle velocities might not be the best way to determine the critical velocity necessary for deposition. Figure 9(b) displays the measured velocity distribution curves for deposition efficiencies of 0 (just beginning to deposit), 53, and 95%, corresponding to mean velocities of 495, 652, and 784 m/s respectively on Fig. 9(a). It can be seen that, although the mean particle velocity for incipient deposition is roughly 500 m/s, a critical velocity of about 640 m/s fits the observed data quite well; that is, the 0% curve is almost entirely below this value, the 53% curve is split, and the 95% curve is almost entirely above this value.

The data show that deposition efficiency is a sensitive function of particle impact velocity and particle-substrate composition (Ref 2, 5). Figure 9(c) indicates that the gun-substrate angle (which should be very close to the incident angle of particle impact for thin coatings) also strongly influences the buildup of the

cold-spray coating. An impact angle of 60° resulted in slight erosion of the aluminum substrate. The data for this plot were obtained with a 22 μm copper powder sprayed with 200 °C, 2.1 MPa (300 psi) helium, giving a velocity magnitude of 649 m/s as measured at a central axis standoff of 25 mm. Because this is very close to the hypothetical critical velocity for deposition, the drop-off in deposition efficiency with substrate angle might be less severe for higher velocity jets. Figure 9(d) replots the data from Fig. 9(c) as a function of the normal velocity component. Also shown in this figure is the corresponding data range for normal impact angle deposition from Fig. 9(a). The divergence of the curves in Fig. 9(d) indicates that while the primary cause of decreasing deposition efficiency with increasing impact angle is the decrease in the normal velocity component, other factors might have a significant influence at low velocities.

No qualitative differences were observed in coatings made with the two different copper powder lots. Particle velocities were somewhat higher for the 19 μm powder than for the 22 μm powder, which resulted in slightly higher deposition efficiencies. However, all of the previously enumerated trends for particle velocity and deposition efficiency as functions of processing parameters are equally valid for either powder size cut.

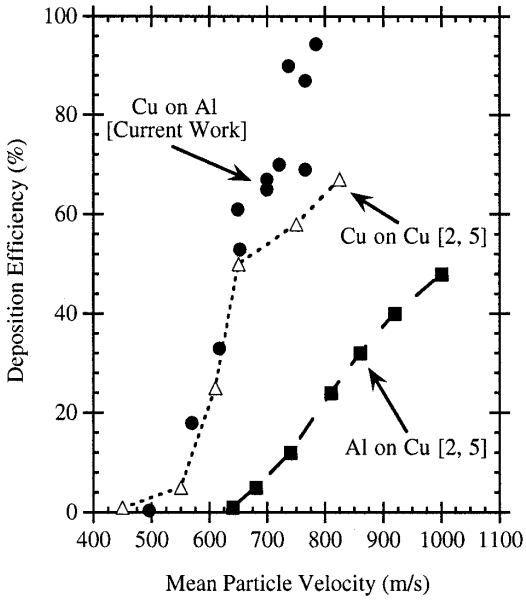

(a)

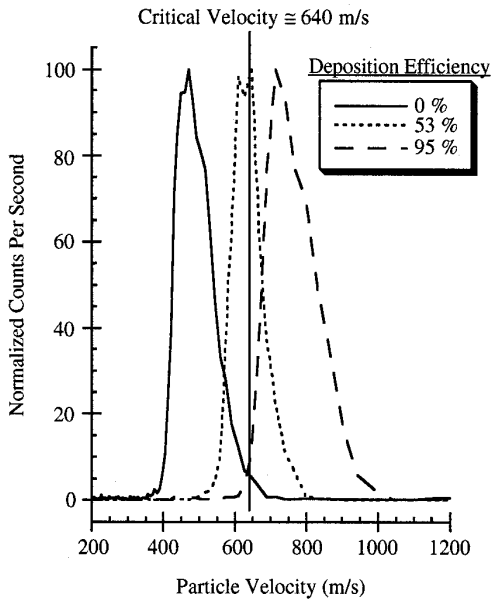

(b)

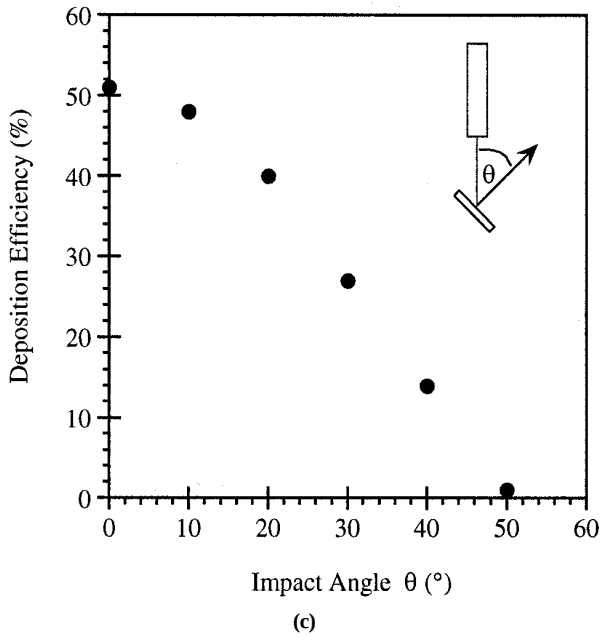

(c)

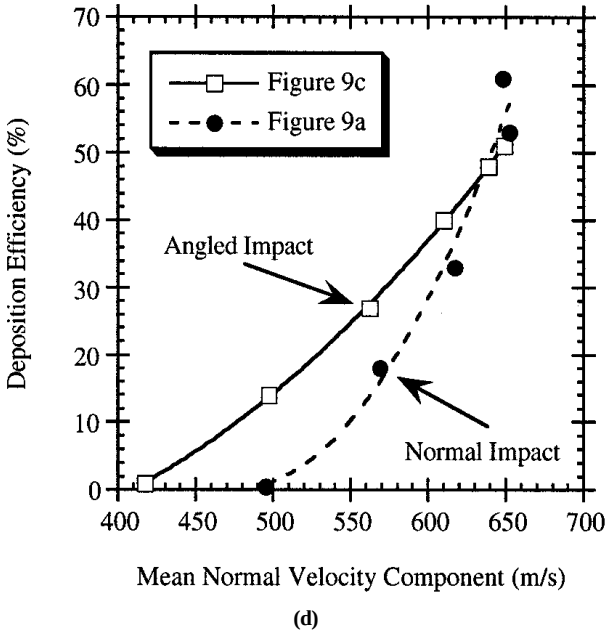

(d)

Fig. 9 (a) Deposition efficiency versus mean particle velocity (x = 0, y = 0, z = 25 mm). 19 μm copper powder, helium driving gas, varying pressure and temperature. (b) Particle velocity distributions corresponding to three different data points from (a) for copper on aluminum. (c) Deposition efficiency versus impact angle (z = 25 mm at central axis); 22 μm copper powder; 200 °C, 2.1 MPa (300 psi) helium driving gas. (d) Deposition efficiency versus normal velocity (z = 25 mm). Data calculated from (c) (angled impact) plotted with corresponding range from (a) (normal impact)

4. Conclusions

This work investigates both the in-flight characteristics of copper particles in a supersonic cold-spray plume and the buildup of the subsequent coating on aluminum substrates. Mean particle velocities were found to be relatively constant within a large volume of the plume. Particle counts dropped off sharply away from the central axis. The presence of the substrate was found to have no effect on the in-flight particle velocities shortly before impact. A significant mass-loading effect on the particle velocity was observed; particle velocities began to drop as the mass ratio of powder to gas flow rates exceeded 3%. The measured variation of velocity with gas pressure and pre-heat temperature was in fairly good agreement with theoretical predictions.

Helium can be used as the driving gas instead of air to achieve higher particle velocities for a given temperature and pressure. Coating deposition efficiencies were found to increase with particle velocity and decrease strongly with gun-substrate angle. There did not appear to be any dependence of the deposition efficiency on coating thickness for this system. A critical velocity for deposition of about 640 m/s appears to fit the present data fairly accurately.

Oxide levels were measured to be somewhat lower in the cold-sprayed coatings than in the original copper powders. The cold-spray technique shows promise as a method for the deposition of materials that are thermally sensitive or can experience rapid oxidation under typical thermal spray conditions. High deposition efficiencies are achievable for certain coating-substrate conditions. Work remains to investigate the material and microstructural properties that govern the coating process.

Acknowledgment

The authors acknowledge the work of Amalia Lopez in running the computer simulations of particle drag used to create Fig. 5(b). Ken Eckelmeyer provided the metallography of the copper powder shown in Fig. 2, and Jeffery Reich performed the oxygen analyses of the powder and coatings.

Sandia is a multi-program laboratory operated by Sandia Corporation, a Lockheed Martin Company, for the U.S. Department of Energy under Contract DE-AC04-94AL85000.

References

1. R.C. Dykhuizen, M.F. Smith, D.L. Gilmore, R.A. Neiser, X. Jiang, and S. Sampath, Impact of High Velocity Cold Spray Particles, *J. Therm. Spray Technol.*, Vol 8 (No. 4), 1999, p 559-564
2. P. Alkimov, V.F. Kosarev, and A.N. Papyrin, A Method of Cold Gas-Dynamic Deposition, *Sov. Phys. Dokl.*, Vol 35 (No. 12), 1990, p 1047-1049, translation American Institute of Physics, 1991
3. A.P. Alkimov, A.N. Papyrin, V.F. Kosarev, N.I. Nesterovich, and M.M. Shuspanov, Gas Dynamic Spraying Method for Applying a Coating, U.S. patent 5,302,414, 12 April 1994
4. A.O. Tokarev, Structure of Aluminum Powder Coatings Prepared by Cold Gas-Dynamic Spraying, *Met. Sci. Heat Treat.*, Vol 38 (No. 3-4), 1996, p 136-139
5. R.C. McCune, A.N. Papyrin, J.N. Hall, W.L. Riggs, and P.H. Zajchowski, An Exploration of the Cold Gas-Dynamic Spray Method for Several Materials Systems, *Advances in Thermal Spray Science and Technology*, C.C. Berndt and S. Sampath, Ed., ASM International, 1995, p 1-5
6. R.C. McCune, W.T. Donoon, E.L. Cartwright, A.N. Papyrin, E.F. Rybicki, and J.R. Shadley, Characterization of Copper and Steel Coatings Made by the Cold Gas-Dynamic Spray Method, *Thermal Spray: Practical Solutions for Engineering Problems*, C.C. Berndt, Ed., ASM International, 1996, p 397-403
7. T.H. VanSteenkiste et al., Kinetic Spray Coatings, *Surf. Coat. Technol.*, Vol 111, 1999, p 62-71
8. R.C. Dykhuizen and M.F. Smith, Gas Dynamic Principles of Cold Spray, *J. Therm. Spray Technol.*, Vol 7 (No. 2), 1998, p 205-212
9. M.F. Smith, T.J. O'Hern, J.E. Brockmann, R.A. Neiser, and T.J. Roemer, A Comparison of Two Laser-Based Diagnostics for Analysis of Particles in Thermal Spray Streams, *Advances in Thermal Spray Science and Technology*, C.C. Berndt and S. Sampath, Ed., ASM International, 1995, p 105-110
10. A.R. Lopez, B. Hassan, W.L. Oberkampf, R.A. Neiser, and T.J. Roemer, Computational Fluid Dynamics Analysis of a Wire-Feed, High-Velocity Oxygen-Fuel (HVOF) Thermal Spray Torch, *J. Therm. Spray Technol.*, Vol 7 (No. 3), 1998, p 374-382
11. R.H. Sabersky, A.J. Acosta, and E.G. Hauptmann, *Fluid Flow: A First Course in Fluid Mechanics*, 3rd ed., Macmillan, 1989